A 6.4-GHz Spurious-Free Acoustic Filter based on Lithium Niobate S1-Mode Resonator

Xueyan Liu[#1], Zhongbin Dai[#2], Zijia Su[#3], Chengjie Zuo[#$4]
[#]School of Microelectronics, University of Science and Technology of China, Hefei, China
[$]YUNTA Technologies and ANUKI Technologies, Hefei, China
[1]xueyanliu@mail.ustc.edu.cn, [2]dzb123@mail.ustc.edu.cn, [3]suzijia@mail.ustc.edu.cn, [4]czuo@ustc.edu.cn

***Abstract*—This paper reports on a 6.4-GHz spurious-free filter based on first-order symmetric (S1) mode resonator fabricated in X-cut lithium niobate (LN) thin film. Specifically, we studied the electrode pitch and duty factor (DF) to suppress parasitic modes near the target resonant frequency, making it possible to better meet the requirements of spurious-free and fast roll-off in a filter. The fabricated resonator has an electromechanical coupling coefficient (k^2) of 3.3% and a high quality factor (Q) of 989, while the filter exhibits low insertion loss (IL) of 2.6 dB and sharp roll-off from 2.6 dB to 40 dB within a narrow transition band of only 55 MHz (out of 6.4 GHz center frequency). The spurious-free filter design opens the possibility of S1-mode LN resonators for filter synthesis in 6G and Wi-Fi 7 applications.**

***Keywords*—S1 mode, lithium niobate, 6G, acoustic resonator, acoustic filter, spurious mode.**

I. Introduction

Due to the ever increasing congestion in the electromagnetic spectrum below 6 GHz, the FCC released a new frequency band (5.945-7.125 GHz) for unauthorized use in April 2020 and many countries have already put forward a series of research projects to explore applications in this band [1]. As frequencies rise and system requirements become more stringent, carrying out high-performance radio frequency (RF) acoustic devices has become a priority. One of the key technologies is to design spurious-free and high quality-factor (Q) acoustic resonators above 6 GHz, which enables sharp roll-off and prevents cross interference between the 6G and Wi-Fi bands [2].

Recently, as heterogeneous integration and layer transfer technology develop, single-crystal lithium niobate ($LiNbO_3$ or LN) thin films with exceptional piezoelectric properties have become very popular for electromechanical and acousto-optic research [3]. At the same time, different cut angle of LN films (X-cut, Y-cut or Z-cut) provides more freedom to customize material and device characteristics. Novel surface acoustic wave (SAW) devices have recently been realized based on this kind of piezoelectric on insulator (POI) material, but the operating frequency is still limited below 5 GHz [4]. Therefore, the design of Lamb wave resonators based on LN for high frequencies has become a research hotspot.

In the past, researchers focused on the antisymmetric Lamb wave modes (A1, A3, etc.), with less attention on the symmetric (S1, S3, etc.) modes that possess high acoustic velocity [5]-[7]. Additionally, previous studies concentrate on the improvement of Q_s, whereas the significance of Q_p in filter design is rarely mentioned [8]. Recently it has been demonstrated that S1-mode resonators based on X-cut LN films can have ultra high Q_p [2], which can both improve the isolation of duplexers and bring steep roll-off for RF filters.

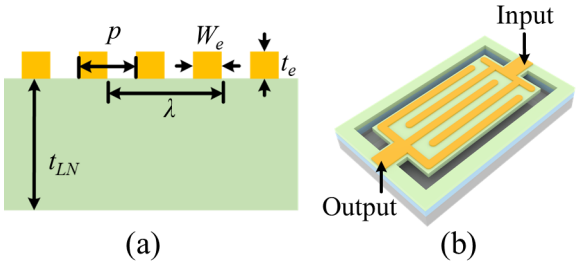

Fig. 1. Schematic diagram of the resonator structure: (a) cross-section view of the resonator; (b) illustration of the suspended resonator.

However, the presence of complex parasitic modes near S1 mode can be fatal for filter design because they create unwanted ripples in the filter transmission curve, which impedes the development of S1-mode devices. Researchers have proposed many strategies for spurious mode suppression: for example, using different electrode shapes [9], electrode apodization [10], adjusting the aperture length [11] and etc. However, the complexity of Lamb wave modes and the anisotropy of X-cut LN film necessitate further study on efficient suppression techniques, which must also be practical for filter design.

Aiming to prove the enormous potential of the S1 mode in 6G mobile communications, this work first designed an in-band spurious-free resonator that can be applied to filter design by studying the influence of electrode pitch and duty factor (DF). The resonator working around 6.4 GHz has a Q of 989 and a k^2 of 3.3%. It has also been demonstrated that a 6.4-GHz ladder-topology acoustic filter has low insertion loss of 2.6 dB, close-in notch rejection of 40 dB, in-band ripple of less than 0.5 dB, and bandwidth of 84 MHz. The high frequency, spurious-free and sharp roll-off characteristics of S1-mode filters show great potential for 6G and Wi-Fi 7 applications.

II. Characteristics of S1 Mode in X-Cut LN Film

In this study, X-cut LN film on SiO_2/Si composite substrate is used for acoustic device fabrication. Fig. 1 (a) depicts a cross-section view of the two-port S1-mode resonator. Fig. 1 (b) illustrates the resonator consisting of top interdigitated transducers (IDTs) and suspended LN film, and the S1 mode can be effectively excited by applying horizontal electric field. The geometrical parameters of the fabricated resonator are as follows: p is 15 μm, W_e is 5 μm, t_e is 20 nm, and Au is chosen as electrode material because of its excellent conductivity and

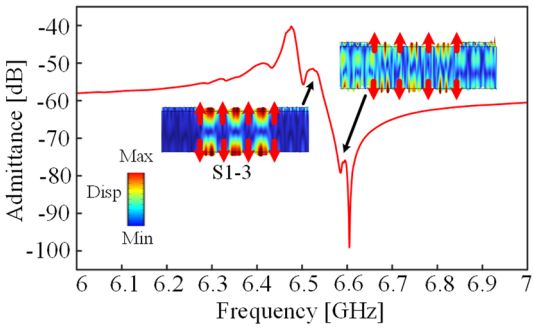

Fig. 2. Admittance curve from measurement of resonator indicating spurious modes

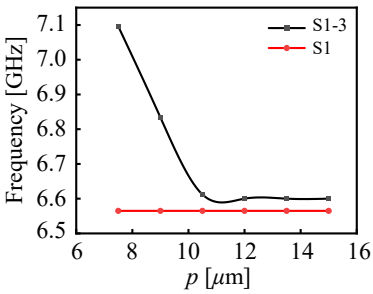

Fig. 3. The resonant frequency plotted as a function of electrode pitch for S1 and S1-3 modes.

low loss. To reach the target high frequency, the LN film is chosen to be 500 nm thick.

Fig. 2 describes the measured admittance curve of the S1-mode resonator whose resonant frequency is around 6.4 GHz. It shows k^2 of 4.7%, Q_s of 279, and Q_p of 5,504. In spite of its high frequency and high Q, the measurement curve shows that this resonator contains many spurious modes close to the resonant frequency. The spurious modes are mainly generated by the higher-order lateral modes, the shapes of which are simulated using COMSOL® two-dimensional (2D) finite element model (FEM) method as in Fig. 2. Since the vibration amplitude of the lateral S1-3 mode (which is near f_s.) is relatively higher, which will cause significant in-band ripple in filter design, we will mainly study the characteristics of S1-3.

Although the S1 mode is primarily thickness defined, the simulation results show that there are still some spurious modes in the lateral direction. This is due to inhomogeneous electric fields that generate higher-order modes in the transverse direction [12]. Therefore, it is important to study the size of the free piezoelectric region and the area covered by metal electrodes for spurious mode suppression.

III. LN Device Design

A. Impact of Pitch

We notice an effect of electrode pitch (p in Fig. 1) on the resonant frequency of spurious modes for a given thickness of LN film and Au electrodes. Higher-order lateral modes, such as the S1-3 mode, are mainly created by the nonuniform electric field in the lateral X direction (as shown in Fig. 2).

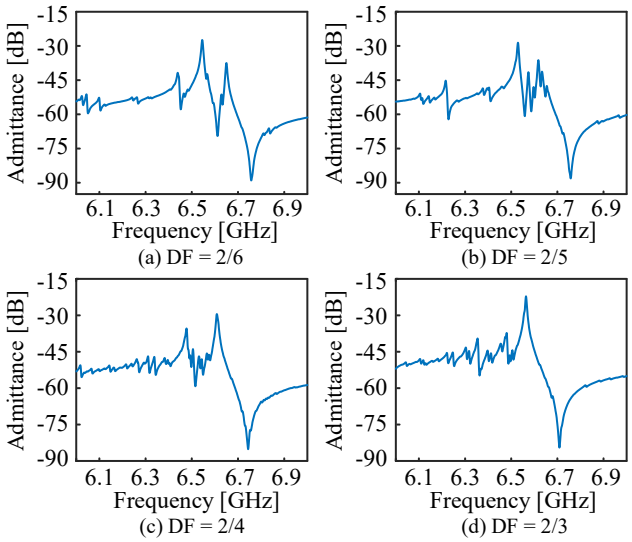

Fig. 4. Simulated admittance curves of S1 Lamb wave mode resonators with varied DF: (a) DF=2/6; (b) DF=2/5; (c) DF=2/4; (d) DF=2/3.

Table I. Design Parameters of the LN S1 Resonators

Design parameter	Value
Thickness of LN [nm]	500
Thickness of Au [nm]	20
DF (Duty Factor)	2/6, 2/5, 2/4, and 2/3
No. of IDTs	5

Fig. 3 displays the simulation results of the S1 mode's dependence on the pitch p. Obviously, the S1-3 shows stronger dependence on the pitch p. The difference in resonant frequency between the two modes significantly increases for pitches under 10 μm, saturating at larger pitches.

B. Impact of Duty Factor

In this section, we discuss the impact of metallization on spurious modes. Typically, the duty factor (DF) or metallization ratio is defined as the ratio of the electrode width (W_e) to the pitch (p), where W_e and p are shown in Fig. 1 (a).

The pitch is set as a constant of 7.5 μm in 2-D finite element simulations, while the electrode width varies. The 2D FEM simulations are used to assess four configurations with DFs of 2/6, 2/5, 2/4, and 2/3, and Table I lists the additional design parameters.

The simulated responses of the four S1 Lamb wave mode resonators are plotted in Fig. 4. With an increase of DF, the spurious mode's vibration frequency gradually drifts away from f_s and f_p, and its vibration amplitude also gradually decreases. By varying the DF, the undesirable modes can be effectively suppressed, since the DF affects the uniformity of electric field and wave numbers of the periodic electrode structure [12]. Finally, the spurious modes are completely suppressed in the passband when DF is 2/3, which is helpful for filter design.

C. 6.4-GHz Acoustic Filter Design

Spurious-free resonators in the passband make filter design easier. The filter in Fig. 5 employs a simple ladder topology

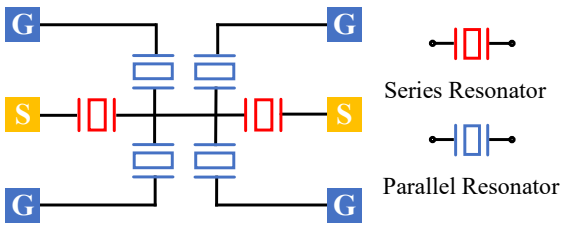

Fig. 5. Circuit schematic showing Ladder topology of the filter.

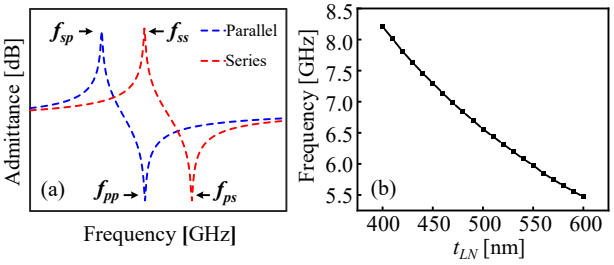

Fig. 6. (a) The admittance of the series and parallel resonators; (b) Relation between the resonant frequency and the LN film thickness.

with four identical parallel resonators and two identical series resonators. The parallel resonators are distributed evenly on both sides of the series resonators to ensure good reciprocity.

To obtain the frequency shift between series and parallel resonators as required in the Ladder topology, partial etching of the LN film is performed in the area where series resonators sit, as shown in Fig. 6 (a). And Fig. 6 (b) shows the relation between the resonant frequency and the thickness of the X-cut LN film. Arrays of resonators electrically connected in parallel are used to lower the device impedance to realize 150 Ω termination. Table II lists the specific design parameters of the series and parallel resonators, as indicated in Fig. 5. C_0 and L are the static capacitance of the resonator array and the length of the resonator aperture, respectively.

Table II. Design Parameters of Series and Parallel Resonators

Parameter	t_{LN} (nm)	W_e (μm)	p (μm)	t_e (nm)	L (μm)	C_0 (fF)
Series arrays	490	5	7.5	20	225	204
Parallel arrays	500	5	7.5	20	225	68

IV. Fabrication and Measurement

A. Fabrication Process

Fabrication process of resonators and the filter is shown in Fig. 7. An Ar_2-based inductively coupled plasma (ICP) method is used to regionally thin 500-nm thick X-cut LN films to 490 nm, and then 20 nm of Au is sputtered as IDTs and connecting lines on the top of the LN film. SiO_2 is chosen as a hard mask to protect IDTs from etching. In step 3, SiO_2 and LN is etched by reactive ion etching (RIE) and inductively coupled plasma (ICP) system to establish the release window. A 7:1 Buffered Oxide Etch (BOE)-based wet etching is used in the final step to

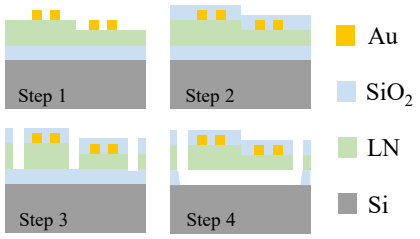

Fig. 7. Fabrication process of the S1-mode X-cut LN devices.

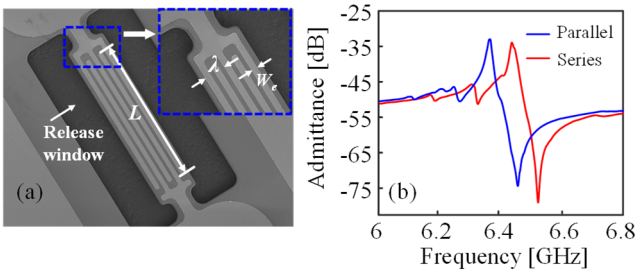

Fig. 8. Results of resonators: (a) scanning electron micrograph (SEM) of the fabricated resonator with its geometry labeled; (b) measured resonator responses in series and parallel branches.

remove the hard mask and sacrificial layer (SiO_2) under the LN thin film, which forms a suspended resonator structure and greatly reduces acoustic energy leakage.

B. Measurement Results

For two-port scattering parameter (S-parameter) testing, Ground-Signal-Ground (GSG) probes with pitch of 150 μm are used, and the sample is mounted on a 12-inch probe station (MPI® TS3000-SE). A vector network analyzer (Keysight® N5227B PNA) is used to measure and record the two-port S parameters of the resonators after the short-open-load-through (SOLT) calibration. The admittance of the device under test (DUT) is further extracted from the S parameters using matrix operation.

1) Results of Resonators

Fig. 8 (a) shows the scanning electron micrograph (SEM) of the fabricated resonator with its geometry labeled, and Fig. 8 (b) shows the admittance curves obtained from the series and parallel resonator tests. Parameters like k^2 and Q are important indicators for assessing resonator performance, where k^2 is calculated as follows [13]:

$$k^2 = \frac{\pi^2}{4}\frac{f_p - f_s}{f_p}. \quad (1)$$

The series resonator's quality factor at parallel resonance (Q_p) is 989, the Q at series resonance (Q_s) is 313, and the k^2 is calculated using Equation (1) to be 3.3%. Similarly, the parallel resonator's Q_s and Q_p have respective values of 429 and 684, and the k^2 is 3.3%. The results also demonstrate the feasibility of the design approach in section III. Compared to the initial resonator test curve as shown in Fig. 2, there are a degree of drop in k^2 and a slight improvement in Q_s, which indicate that there is a trade-off between pitch and k^2. Q_p of the resonator is also adequate in terms of resonator performance in the 6 GHz band, allowing for a steep roll-off of the filter.

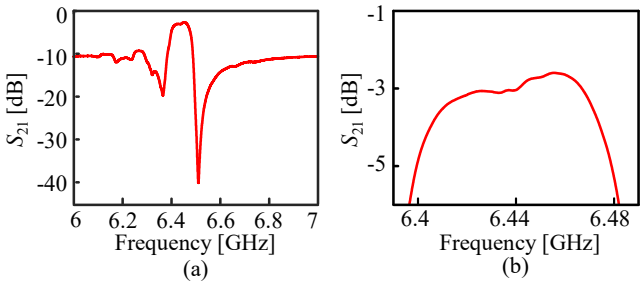

Fig. 9. Measured response of the filter as: (a) S_{21} curve; (b) zoom-in passband response.

2) *Results of the Filter*

The fabricated filter's S_{21} curve is displayed in Fig. 9. The filter has an insertion loss of 2.6 dB of which close-in notch rejection is 20 dB on the left side of the passband and 40 dB on the right side. The center frequency of the filter is around 6.44 GHz, with a bandwidth of 84 MHz. The in-band ripple is less than 0.5 dB, and the transmission curve is spurious-free in the passband, demonstrating the effectiveness of the resonator design. It is noteworthy that the S_{21} (right side of the passband) drops sharply from 2.6 dB to 40 dB when the frequency changes from 6455 MHz to 6510 MHz (a transition band of 55 MHz), which is attained with a resonator Q_p of 989, highlighting the importance of high Q for upcoming filter designs in mobile communications.

However, due to the capacitive nature of resonators based on the X-cut LN film, the out-of-band rejection far away from the filter passband still needs to be improved to better meet the needs of practical applications, and we plan to use integrated passive devices (IPD) to implement hybrid filter design in order to achieve this goal in future work [14].

V. CONCLUSION

In this work, a 6.4-GHz spurious-free RF filter based on X-cut LN film is designed and fabricated. To effectively suppress the parasitic vibration modes, we carefully design the electrode pitch and DF of interdigital transducers on the MEMS resonator. The fabricated resonator has a high Q close to 1,000, and the k^2 is 3.3%. Based on the high-Q resonators, a 6.4-GHz RF filter is implemented using the Ladder topology, which is the first high frequency (> 6 GHz) S1-mode filter demonstrated todate. This filter has low insertion loss of 2.6 dB, high notch rejection of 40 dB and sharp roll-off, which proves its great potential in 6G and Wi-Fi 7 applications to provide sharp isolation between neighbouring high-frequency bands.

ACKNOWLEDGMENT

This work was supported in part by the National Key Research and Development Program of China under Grant 2020YFB2008803, in part by the Fundamental Research Funds for the Central Universities under Grant WK2100230020, in part by the USTC Center for Micro and Nanoscale Research and Fabrication, and in part by the USTC Institute of Advanced Technology.

REFERENCES

[1] Report and Order and Further Notice of Proposed Rulemaking, Federal Commun. Commission, Washington, DC, USA, Apr. 2020, pp. 20–51.

[2] Z. Dai, X. Liu, H. Cheng, S. Xiao, H. Sun and C. Zuo, "Ultra High Q Lithium Niobate Resonator at 15-Degree Three-Dimensional Euler Angle," *IEEE Electron Device Lett*, vol. 43, no.7, pp. 1105-1108, July 2022.

[3] Y. Shuai et al., "Fabrication of Y128- and Y36-cut lithium niobate single-crystalline thin films by crystal-ion-slicing technique," *Jpn. J. Appl. Phys.*, vol. 57, no. 4S, Apr. 2018.

[4] H. Xu et al., "Large-Range Spurious Mode Elimination for Wideband SAW Filters on $LiNbO_3/SiO_2/Si$ Platform by $LiNbO_3$ Cut Angle Modulation," *IEEE Trans. Ultrason. Ferroelectr. Freq. Control*, vol. 69, no. 11, pp. 3117-3125, Nov. 2022.

[5] Y. Yang, R. Lu, L. Gao and S. Gong, "4.5 GHz Lithium Niobate MEMS Filters With 10% Fractional Bandwidth for 5G Front-Ends," *J. Microelectromechanical Sys*., vol. 28, no. 4, pp. 575-577, Aug. 2019.

[6] S. Link, R. Lu, Y. Yang, A. E. Hassanien and S. Gong, "An A1 Mode Resonator at 12 GHz using 160nm Lithium Niobate Suspended Thin Film," *2021 IEEE International Ultrasonics Symposium (IUS)*, 2021, pp. 1-4.

[7] R. Lu, Y. Yang, S. Link and S. Gong, "Low-Loss 5-GHz First-Order Antisymmetric Mode Acoustic Delay Lines in Thin-Film Lithium Niobate," *IEEE Trans. Micro. Theory. Tech*, vol. 69, no. 1, pp. 541-550, Jan. 2021.

[8] R. Vetury et al., "High Rejection, 160MHz Bandwidth, High Q-factor 6 GHz RF Filters for Wi-Fi 6E manufactured in a Novel BAW Process," *2021 IEEE International Ultrasonics Symposium (IUS)*, 2021, pp. 1-4.

[9] J. Liu et al., "Lithium Niobate Film Based Acoustic Wave Resonator with Arc Shaped Electrodes," *2021 IEEE International Ultrasonics Symposium (IUS)*, 2021, pp. 1-3.

[10] H. Iwamoto, T. Takai, Y. Takamine, T. Nakao, T. Fuyutsume and M. Koshino, "Transverse Modes in I.H.P. SAW Resonator and Their Suppression Method," *2018 IEEE International Ultrasonics Symposium (IUS)*, 2018, pp. 1-4.

[11] S. Wu, Z. Wu, F. Bao and J. Zou, "High-Q Resonator–Inductor Using $LiNbO_3$ Plate for Frequency Tuning in 1–5 GHz," *IEEE Trans. Ultrason. Ferroelectr. Freq. Control*, vol. 69, no. 7, pp. 2331-2338, July 2022.

[12] S. Yandrapalli, V. Plessky, J. Koskela, V. Yantchev, P. Turner and L. G. Villanueva, "Analysis of XBAR resonance and higher order spurious modes," *2019 IEEE International Ultrasonics Symposium (IUS)*, 2019, pp. 185-188.

[13] R. Lu, M. -H. Li, Y. Yang, T. Manzaneque and S. Gong, "Accurate Extraction of Large Electromechanical Coupling in Piezoelectric MEMS Resonators," *J. Microelectromechanical Sys*., vol. 28, no. 2, pp. 209-218, April 2019.

[14] C. Zuo, C. He, W. Cheng and Z. Wang, "Hybrid Filter Design for 5G using IPD and Acoustic Technologies," *2019 IEEE International Ultrasonics Symposium (IUS)*, 2019, pp. 269-272.